

References

Burckhardt CB, Speckle in ultrasound B-mode scans. IEEE Trans Sonics Ultrason 1978; 2: 1-6

Tuthill TA, Sperry RH, Parker KJ. Deviations from Rayleigh statistics in ultrasonic speckles. Ultrason Imaging 1988; 10: 81-89

Yamada H, Ebara M, Yamaguchi T, et al. A pilot approach for quantitative assessment of liver fibrosis using ultrasound: preliminary results in 79 cases. J Hepatol 2006; 44: 68-75

Toyoda H, Kumada T, Kamiyama, N et al. B-Mode Ultrasound With Algorithm Based on Statistical Analysis of Signals: Evaluation of Liver Fibrosis in Patients With Chronic Hepatitis C. AJR 2009; 193:1037-1043

TOSHIBA

Leading Innovation >>>

Acoustic Structure Quantification (ASQ) – A new diagnostic tool in ultrasonography of the liver

Prof. Dr. med. Jörg Bleck

Medical Director, Ultrasound Center,
Johanniter Krankenhaus Genthin-Stendal

Over the last decade methods to quantify the changes of ultrasonic texture have focussed on non-invasive tissue classification of parenchymal organs – primarily the liver – by using different mathematical procedures. Despite excellent reclassification results, these procedures, however, never achieved clinical significance because they lack standardization, they strongly depend on the signal processing and in everyday routine the measured parameters are difficult to visualize. Nevertheless, quantitative procedures to measure elasticity have gained importance particularly with regard to the quantification of liver fibrosis. In addition, recognition, quantification and follow-up of fatty livers are of clinical concern.

Historically, Rayleigh scattering, discovered by Lord Rayleigh, provides the base of ASQ (Acoustic Structure Quantification). It describes the elastic scattering of light that passes gas atoms which have a much smaller diameter than the wavelength of the light. Normal liver parenchyma is mainly composed of a 3D arrangement of many structures that are smaller than the wavelength of the typical ultrasound pulse used in clinical examinations. The statistics of the echo amplitudes in a normal liver fit the Rayleigh probability density function (Burckhardt 1978, Tuthill 1988). In livers containing fibrosis or cirrhosis, nodules and fibrous structures are larger than the ultrasound wavelength. ASQ measures the difference between this

theoretical echo amplitudes distribution and the real measurement in a ROI of a patient, using the chi-square test as statistical tool (Yamada 2006). The results of this comparison, the C_m^2 values, are shown in histogram form (Fig. 5), first order statistics or visually as a coloured look-up table. In order to achieve a high resolution of 15 bit and 100 samples/mm the data are acquired by a raw data interface of the Aplio XG.

Qualitative visual results

As a first step it had to be evaluated whether ASQ provides new information regarding structures that are invisible in the B mode image. Fig. 1 shows a cystic phantom representing sound field

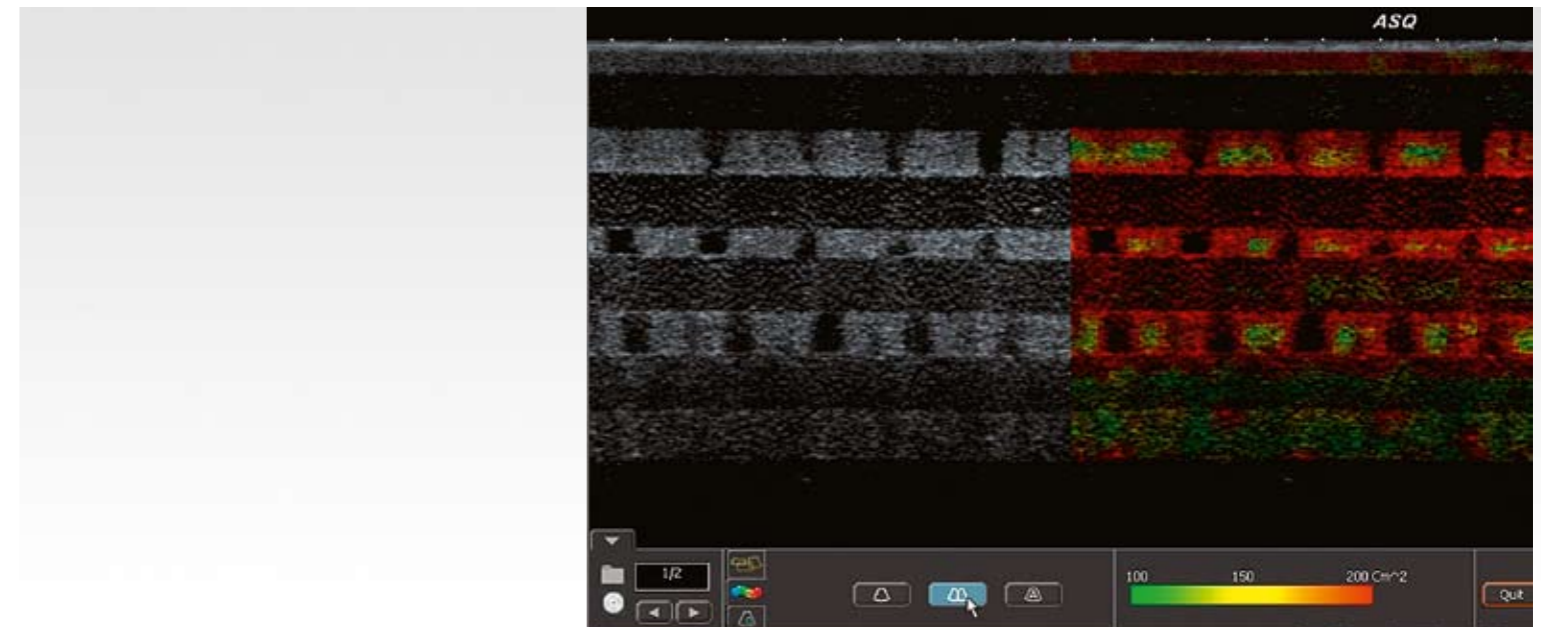


Fig. 1: 3D cyst phantom (QC-180, TCC, Satrapa et al.) depicting conventional greyscale images on the left and ASQ on the right. The pale green C_m^2 values are particularly invisible in the original. They originate from spatial interaction of non-visible cysts adjacent to solid tissue parts of the phantom.

TOSHIBA MEDICAL SYSTEMS CORPORATION

©Toshiba Medical Systems Corporation 2010 all rights reserved.
Design and specifications subject to change without notice.
03/2010 TWPUS0007EC.EU

www.toshiba-medical.eu



ULTRASOUND CT MRI X-RAY SERVICES

interactions of neighbouring invisible cysts.

Other examples of morphological structures, not visible in B mode images, can be demonstrated in the liver. Using a red marker of the medium C_m^2 values (Fig. 2), a mesh-like pattern arises. Yamada et al. (2006) investigated 3D reconstructions of C_m^2 values interpreting the net-like structure as fibrosis providing information of connective tissue representing the increment of fibre and nodules being observed in chronic hepatitis or in cirrhosis. Colouring the more intensive C_m^2 values, homog-

enously distributed vessels with nearly equal distances are depicted with a broad surrounding margin (Fig. 2 and Fig. 3). Both effects are not visible in the original image.

Our first results of the spatial arrangement of vascular structures using yellow/red colour-codes for intensive C_m^2 values show (Fig. 4) that unlike healthy and fatty livers with equal vessel distances, cirrhosis is characterized by irregular distances. Additionally, fibrosis produces a high C_m^2 value

which is particularly visible in scar regions of cirrhotic livers. The normal liver shows higher C_m^2 values around clearly visible lumina, whereas fatty liver produces lower C_m^2 values with yellow coloured, smaller and hardly detectable lumina. In cirrhotic tissue the vascular edges differ in intensity. In focal lesions such as metastasis the halo regions also produce high C_m^2 values (Fig.6).

Quantitative results

In pilot studies Yamada et al. (2006) and Toyoda

et al. (2009) investigated patients with chronic hepatitis C. Both groups postulated a greater potential of diagnosing liver fibrosis using ASQ in ultrasound. However, different fibrosis stages showed a huge overlap. Our preliminary results based on 90 patients (normal liver, fatty liver, end-stage alcoholic cirrhosis) show that the highest C_m^2 values are observed in normal livers, followed by alcoholic cirrhosis and fatty livers (Fig.7). All groups were significantly different. Unlike Yamada et al., who found no significant influence of the

degree of inflammation or steatosis, we must postulate that steatosis produces significant changes of C_m^2 values.

In conclusion ASQ is a promising and powerful tool providing quantitative and qualitative non-invasive analyses of parenchymal organs, e.g. for the detection of cirrhosis and fatty livers.

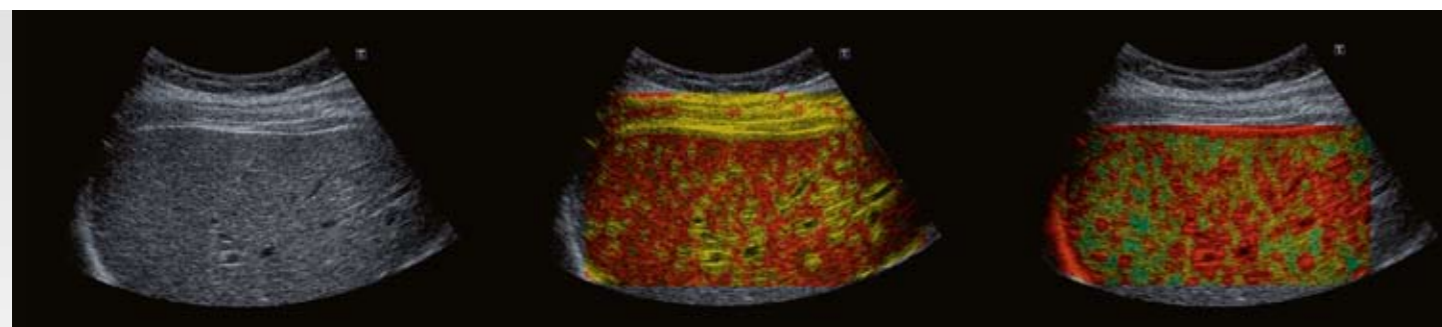


Fig. 2: Normal liver in ASQ greyscale mode (left). In ASQ mode a mesh-like structure of medium C_m^2 values is displayed in red (middle), while the more intense C_m^2 values on the right highlight the margins surrounding the vessels.

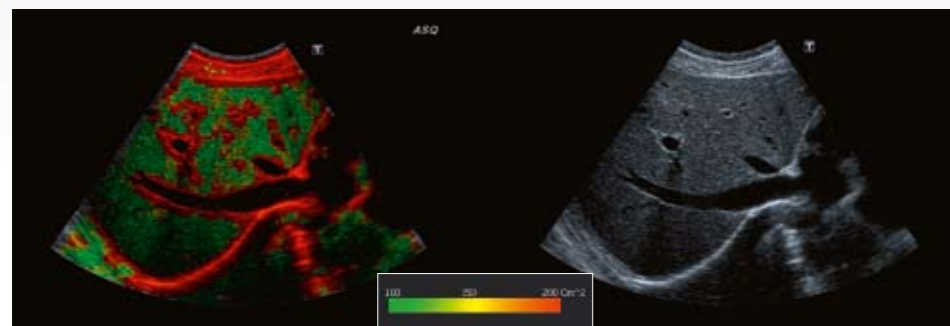


Fig. 3: Subcostal view of the liver without (right) and with ASQ (left). The vascular bed of the portal vein and the liver veins is highlighted (red) whereas the parenchyma shows low C_m^2 values (green). The vessel lumina remain black.

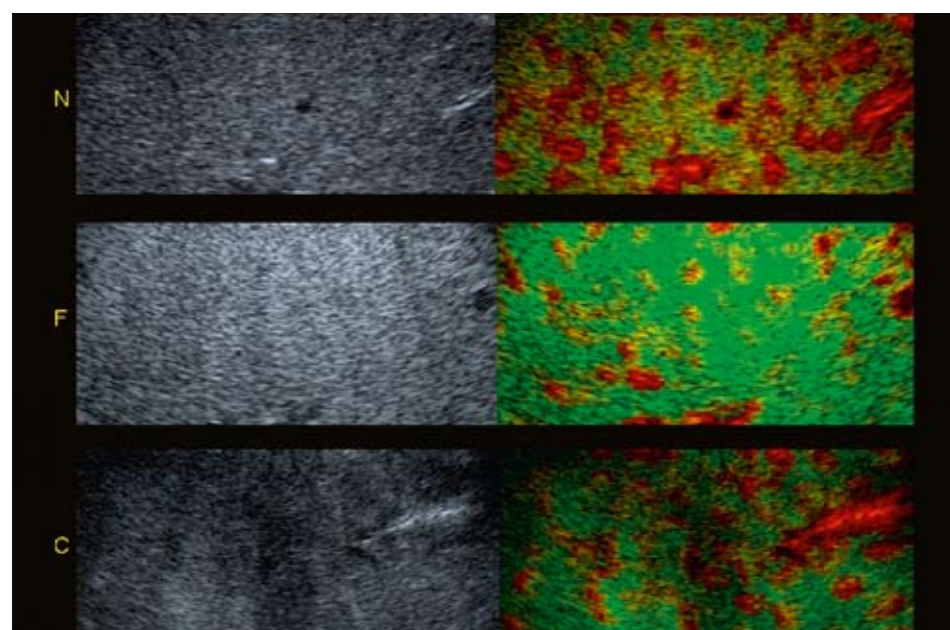


Fig. 4: The left images show native normal liver (N), fatty liver (F) and cirrhosis (C), the right images the coloured C_m^2 values. The distance between the vessels is regular in normal and fatty liver but irregular in cirrhosis. In fatty liver the margin of the vessel shows only low C_m^2 values.

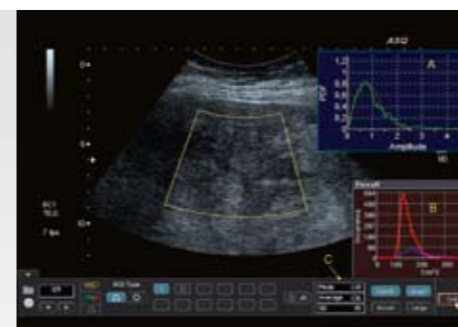


Fig. 5: Example of quantitative tools of C_m^2 values by ASQ. The probability density function PDF of the C_m^2 values (green line) measured in a ROI is displayed against the theoretical speckle generated by Rayleigh distribution (red line) in A. The difference between both is shown as histogram (red line) in B, and the first order statistics of these histograms shown in C (mode, average and standard deviation).

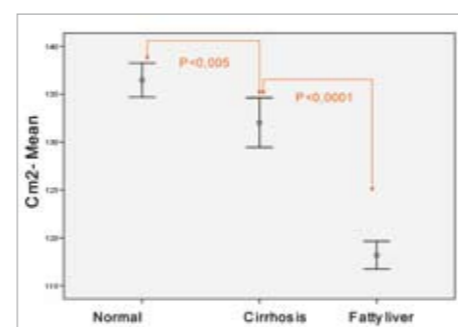


Fig. 7: Display of the mean C_m^2 values of 90 patients (normal, alcoholic cirrhosis, fatty liver) with Tukey HSD test.

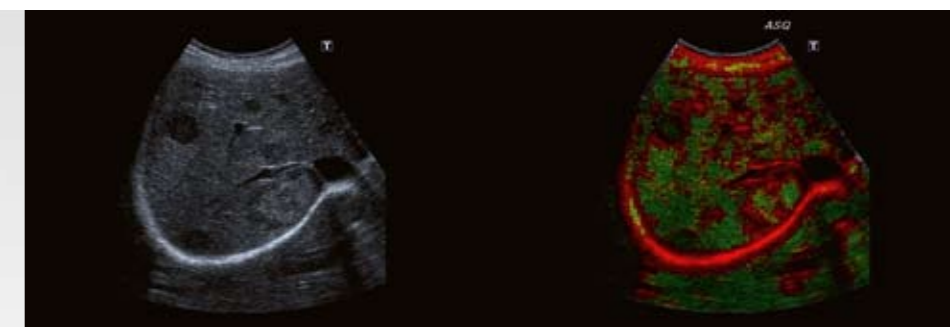


Fig. 6: Metastasis of a mamma carcinoma in the liver. The halo region produces an enhanced ring of C_m^2 values around the lesion.

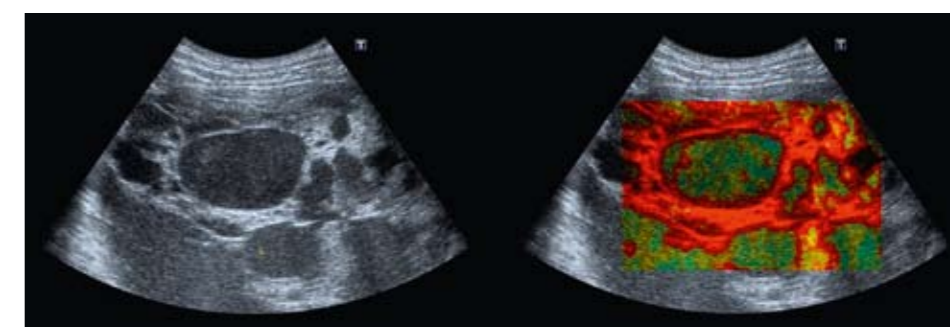


Fig. 8: Example for a pseudomyxoma peritonei. In the ASQ transformation (right) a septum within the cyst appears, invisible in the original (left).